34th AIAA Plasmadynamics and Lasers Conference
23-26 June 2003, Orlando, Florida

AIAA 2003-3859

Energy conversion efficiency of laser produced plasma in a supersonic flow

Koichi Mori [1], Kimiya Komurasaki [2], Hiroshi Katsurayama [3], and Yoshihiro Arakawa [4]

The university of Tokyo, Hongo 7-3-1 Bunkyo 113-8656, Japan

Abstract

The blast wave energy conversion efficiency defined as the fraction of the input laser energy that is converted into the bulk energy of gas motion in the blast wave was measured in the standard atmosphere and the in a M=2 flow. The ambient air pressure, density, input laser energy, and f-number of focusing optics were chosen as parameters. As a result, the blast wave energy conversion efficiency was found to decrease with the ambient pressure, and insensitive to all the other parameters.

Introduction

Laser ramjet and scramjet are the air-breathing laser propulsion, [1-3] which generate thrust without loading propellant on the vehicle. Estimation of the high-altitude performance of the laser ram / scramjet is a key issue for the feasibility study of laser propelled launcher.

A Repetitively pulse (RP) laser ramjet is illustrated in Fig. 1. A pulse Laser beam transmitted remotely from the ground is focused in a flow introduced from an intake. Breakdown occurs in the vicinity of focus, and the laser energy is absorbed efficiently by the Laser Supported Detonation (LSD) wave propagating from the focus in the direction opposite to the laser beam incidence along the laser light channel. [4] The absorbed energy is utilized to drive a blast wave, which is blown down stream imparting an impulsive thrust to a nozzle wall.

The performance of the RP laser ram / scramjet is determined by the global energy balance in producing a blast wave, which can be represented by the blast wave energy conversion efficiency η_{bw} defined as the fraction of the input laser energy that is converted into the blast wave energy. Here, the blast wave energy is defined as the bulk energy of gas motion in the region behind the shock wave:

$$E_{bw} \equiv \int_{V_{bw}} \left(\frac{p - p_a}{\gamma - 1} + \frac{1}{2} u^2 \right) dV \cdot \qquad (1)$$

Energy flow from the laser energy to the blast wave energy is illustrated in Fig. 2. E_{bw} is degraded by radiative energy dissipation and ionization energy frozen in the plasma.

Most research efforts [5-7] concerning the energy conversion in a supersonic flow have been devoted to the quasi-stationary phenomena except for the experimental study by Woodroffe et al. [8] In their experiment, 200-J-laser pulse was irradiated onto an aluminum target placed parallel to a M = 2.8 flow. The impulse density imparted to the target in the flow was found twice as high as in the quiescent air. However, the detailed energy conversion processes have not been clarified until today.

In this study, a focused pulse laser beam was introduced in a M=2 flow, and η_{bw} was measured as a function of the static pressure of the flow. Our interest is the influence of the static parameters of the ambient air on the energy conversion processes.

The effect of the flow was negligibly small in the limit of our experiment, in which the flow velocity was the order of 10^2 m/s, and was much lower than the propagation velocity of the LSD wave in the order of 10^3~10^4 m/s.

---

[1] Graduate student, Department of Advanced Energy, Student member AIAA

[2] Associate professor, Department of Advanced Energy, Member AIAA

[3] Graduate student, Department of Aeronautics and Astronautics

[4] Professor, Department of Aeronautics and Astronautics, Member AIAA

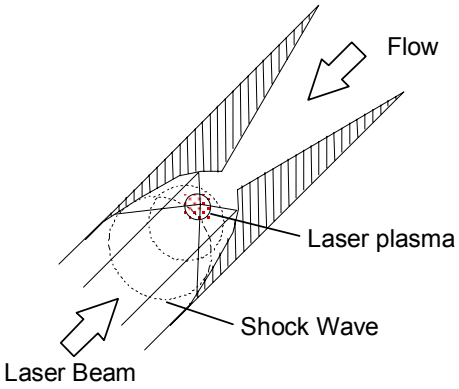

Fig. 1 RP Laser ramjet

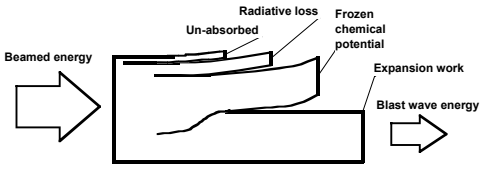

Fig. 2 Energy flow from the input laser pulse to the blast wave energy

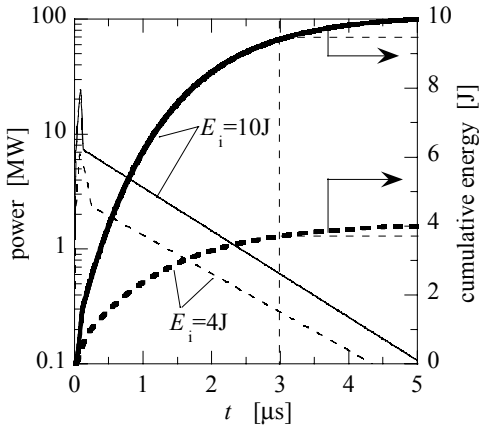

Fig. 3 Laser pulse shape

Table 1 Specifications of the flow

Flow velocity U	512 m/s (M=2)
Total temperature T_0	293 K (room temp.)
Static temperature T_a	163 K
Total pressure P_t	200 – 780 kPa
Static pressure p_a	26 – 100 kPa

Experimental apparatus and methods

Plasma was produced using a TEA CO_2 pulse laser. The input laser energy E_i could be changed from 2 to 12 J. The laser pulse shape, as shown in Fig. 3, was consisted of a leading edge spike and an exponentially decaying tail. More than 95 % of the laser pulse energy has been irradiated until t = 3 μs. Here, t is defined as the elapsed time after the beginning of the laser irradiation.

The laser beam was focused using an off-axial parabola mirror, whose focusing f-number was 2.2. Plasma was produced in the test section of the wind tunnel.

Schematic of the wind tunnel is illustrated in Fig. 4. The focused laser beam was introduced through a Zn-Se window placed at the top wall of the test section, and the laser focus was set 5 mm above the bottom wall. The test section has a 40 square cross section, and 70 mm length along the stream.

Compressed dry air was accelerated by the Raval nozzle to produce an uniform M=2 flow in a test section. The air is exhausted through a diffuser to the atmosphere.

Specifications of the flow in the test section are shown in Table 1. Static pressure of the flow was varied changing the total pressure. It should be especially noted that the air density of the flow was 1.8 times as high as in the quiescent air at the same air pressure because the total temperature of the flow was equal to the room temperature 293 K.

Blast wave pressure was measured using piezo-electoric pressure sensors (Kistler, 603B), which were mounted in the test section ports, which were set along the flow direction every 15 mm.

A schema of shadowgraph system is illustrated in Fig.5. Shadowgraph images were taken using an ICCD camera. The image intensifier was operated as a shutter and an optical emission from the gap-switch of the laser discharge tube was used to trigger the shutter. A He-Ne laser was used as a light source for shadowgraphs.

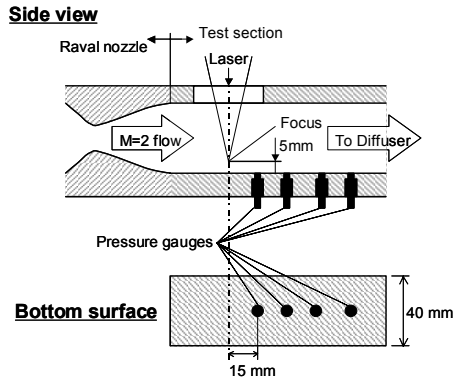

Fig.4 Schematic of the supersonic wind tunnel

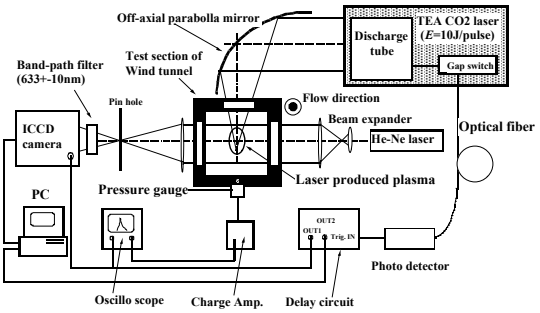

Fig. 5 Schematic of shadowgraph system

Emission from plasma was attenuated selectively by a band-path filter transmitting the wavelength of 633 ± 10 nm. However, observed images were the superposition of the density gradient shadow and plasma luminescence. Since the emission coefficient of bremsstrahlung radiation is proportional to the square of electron density, the emitting region in the images would be identical to the plasma region.

Theory to extract the blast wave energy

According to the self-similar solution of a spherical blast wave, [9] E_{bw} is a function of a volume of blast wave V_{bw} and the Mach number of the expanding shock wave M_s as

$$E_{bw} = \frac{75\gamma}{16\pi\xi_0^{\,5}} p_a V_{bw}(t) M_s^{\,2} \qquad (2)$$

where ξ_0 is constant at 1.03 for air (γ = 1.4). Although the original self-similar solution assumes a spherical expansion of shock wave, Eq. (2) can be applied even to the elliptic blast wave expansion. [10]

Although Eq. (2) assumes an ultimately strong shock wave ($M_s \to \infty$), it can be corrected to apply the finite-strength cases as

$$E_{bw} = p_a V_{bw}(t) f(M_s) \qquad (3)$$

where f (M_s) was obtained from numerical computation results as

$$f(M_s) = AM_s^{\alpha} \qquad A = 6.6983 \qquad \alpha = 2.0433 \qquad (4)$$

as long as $2.0 < M_s < 48.0$. [10]

The laser-induced blast wave shaped elliptically. However, the Mach number became unique during the adiabatic expansion of shock wave. The major radius R_a and the minor radius R_b can be expressed as

$$R_a = R_{a,0} + R(t - t_0) \qquad R_b = R_{b,0} + R(t - t_0) \qquad (5)$$

From Eqs. (3)-(5), an ordinary differential equation is deduced as

$$R_a^{\frac{1}{\alpha}} R_b^{\frac{2}{\alpha}} \frac{dR(t-t_0)}{dt} = c_a \left(\frac{E_{bw}}{Ap_a} \right)^{\frac{1}{\alpha}}, \qquad (6)$$

Here, c_a is the sound speed of the ambient air. Integrating Eq. (6) with t, a linear expression

$$g(R_a, R_b) = c_a \left(\frac{E_{bw}}{Ap_a} \right)^{\frac{1}{\alpha}} (t - t_0)$$

$$g(R_a, R_b) \equiv \frac{1}{1+2/\alpha} R_a^{\frac{1}{\alpha}} R_b^{1+\frac{2}{\alpha}} \left\{ 1 + \left(\frac{R_b}{R_a - R_b} \right) \right\}^{-\frac{1}{\alpha}} \times {}_2F_1 \left[1+\frac{2}{\alpha}, -\frac{1}{\alpha}, 2+\frac{2}{\alpha}; -\frac{R_b}{R_a - R_b} \right] \qquad (7)$$

is obtained. Here, ${}_2F_1$ is a hyper-geometric function.

The value of function $g(R_a, R_b)$ is calculated from measured R_a and R_b in the shadowgraph images. The blast wave energy can be obtained from the inclination $\Delta g / \Delta t$.

Results

Shadowgraph images

Shadowgraph images of laser-produced plasma taken in the M=2 flow are shown in Fig. 6. The LSD wave was observed until t = 2 μs. As was the case in the quiescent air, luminous plasma was left behind a shock wave at t > 2 μs, and the laser heating in the LSD wave has terminated. Although the LSD wave does not influenced by the flow, the explosion center was blown

downstream while the elliptic shock wave expanded further.

Comparing Figs. 6 (a) and (b), the volume of blast wave appeared larger in p_a = 26 kPa than in p_a = 100 kPa due to the reduction in p_a.

Blast wave energy measurement

Typical temporal history of the major and minor radii of the elliptic shock wave is shown in Fig. 7 in the case of the quiescent standard air atmosphere. Deduced Mach number is drawn together in the figure. M_a and M_b correspond to the expansion Mach number of the major and minor radius, respectively. At t > 3 μs, the Mach number in each direction has coalesced to each other.

The corresponding functional value $g(R_a, R_b)$ were calculated from the radii data as shown in Fig. 8(a). $g(R_a, R_b)$ increased accelerating with t until t ~ 3 μs due to the laser heating, and then became to increase linearly. From Δg / Δt measured at the linearly increasing part of g - t plots, E_{bw} was deduced using Eq. (7).

The blast wave energy is plotted against E_i in Fig. 9. E_{bw} increased linearly with E_i, and η_{bw} averaged over the measured range of E_i from 2 to 12 J was found at 0.47±0.05.

In Table 2, η_{bw} data measured with f = 3.3 focusing mirror is comparatively presented. η_{bw} appeared insensitive to the input laser energy and the f-number of the focusing optics.

$g(R_a, R_b)$ deduced from the images taken in the M = 2 flow are shown in Fig. 8 (b). As was the case in the quiescent condition, $g(R_a, R_b)$ increased linearly with t after t ~ 3 μs. Figure 10 shows the relation between η_{bw} and p_a. Despite the difference in the ambient air density, η_{bw} measured in M = 2 flow were quite close to that measured in the quiescent air at the same ambient pressure.

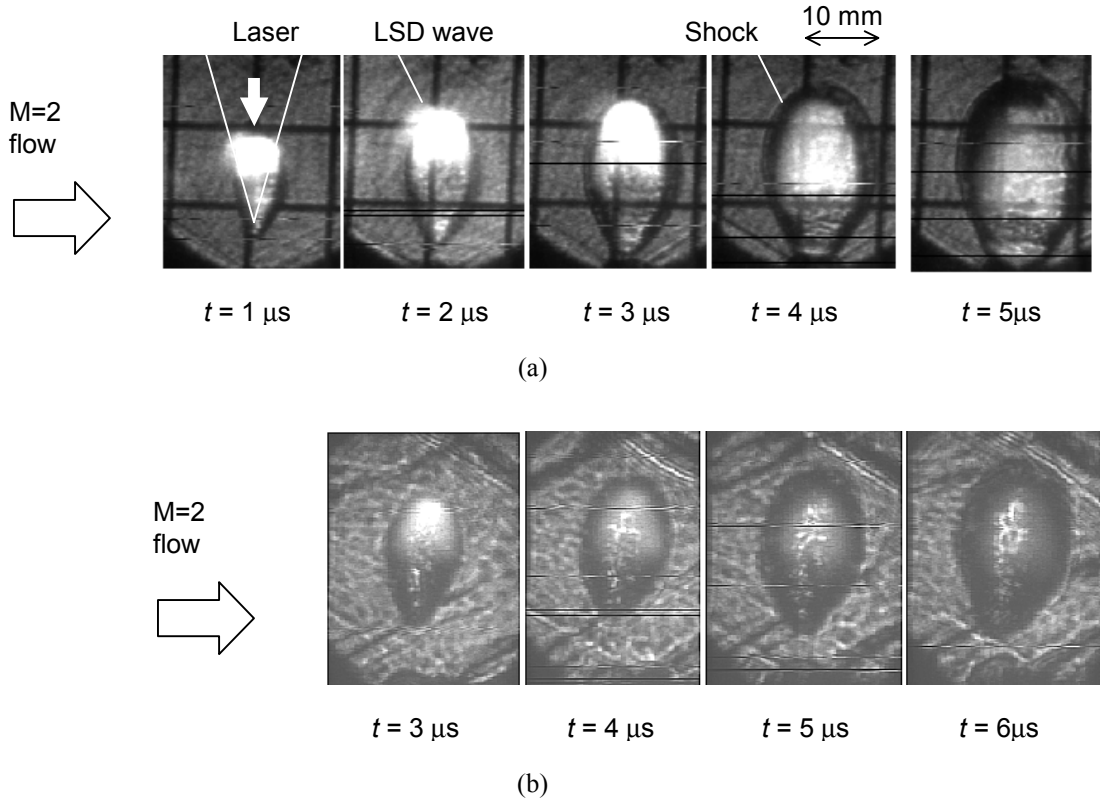

Fig. 6 Shadowgraph images of laser induced blast wave in M=2 flow: (a) with p_a = 26 kPa; (b) with p_a = 100 kPa (standard atmospheric pressure).

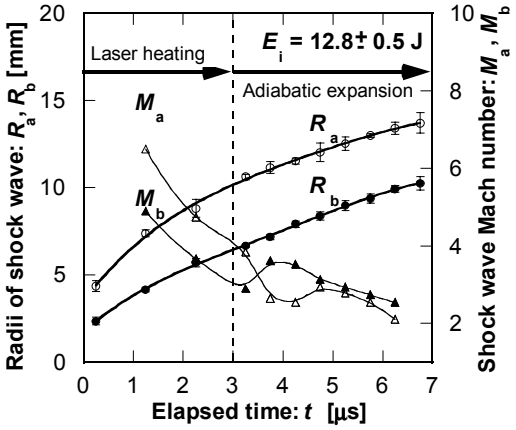

Fig. 7 Temporal variation of shock wave radii and the Mach number in the standard atmosphere

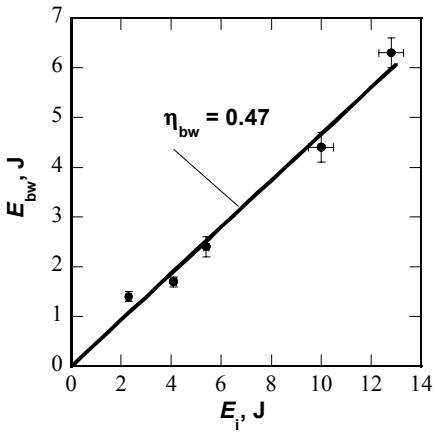

Fig. 9 Blast wave energy conversion efficiency in p_a = 100 kPa quiescent air

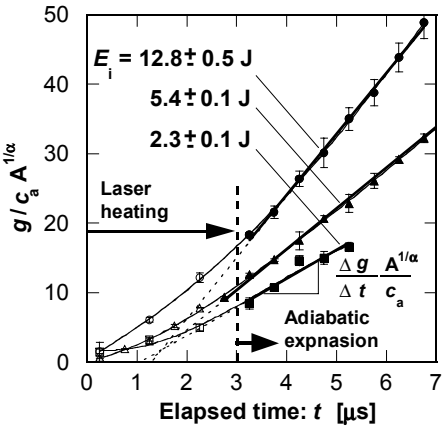

(a)

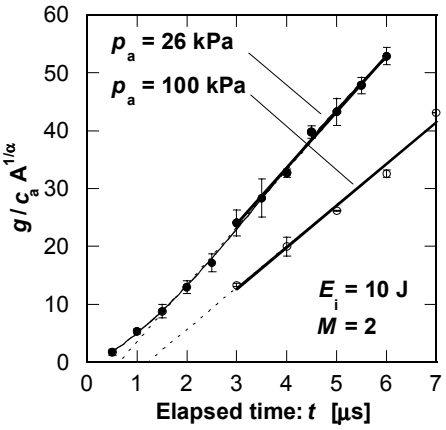

(b)

Fig. 8 Temporal variation of g: (a) in the standard atmosphere; (b) in the M = 2 flow with E_i = 10 J

Table 2 η_{bw} measured under various iput conditions with pa = 100 kPa

f-number	Range of E_i [J]	η_{bw}
2.2	2 - 12	0.47±0.05
3.3	6 - 12	0.44±0.1

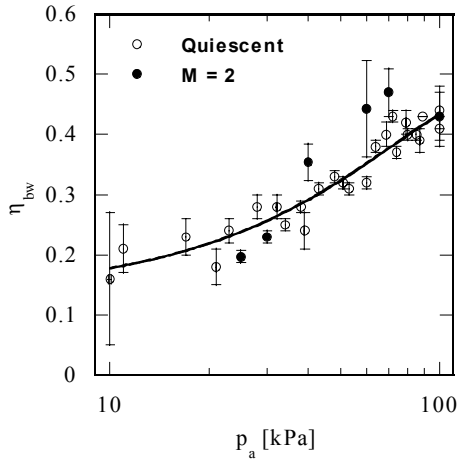

Fig. 10 Relation of the ambient pressure pa to the blast wave energy conversion efficiency.

Pressure measurement

Our results presented in Fig. 10 were verified by the pressure measurement qualitatively. According to the Sedov-Taylor self-similar solution, the maximum over-pressure Δp of the spherical blast wave increases linearly with the blast wave energy as

$$\Delta p \propto E_{bw} / R^3 \qquad (8)$$

where R is the radius of shock wave.

The convection of the explosion center is schematically drawn in Fig. 11. In the M=2 flow, the explosion center is blown down stream with the velocity of the flow: U = 512 m/s (See Table I). Suppose a the shock wave arrives at a pressure sensor mounted at a position X at $t = t_1$, the shock wave radius R is equal to $X - U t_1$.

Typical temporal history of the pressure measured at the bottom surface of the test section is shown in Fig. 12. The maximum over-pressure was recorded at an arrival time.

Figure 13 shows the relation between the maximum over pressure and the shock radius $X - Ut$, where t represents the arrival time of the shock wave. Since E_{bw} in the quiescent air was close to that in the M=2 flow at the same ambient pressure as shown in Fig. 10, Δp in both cases were also close to each other as predicted by Eq. (8). Correspondingly, Δp in p_a = 23 kPa was about half as high as Δp in p_a = 100 kPa due to the decrease in E_{bw}. All these results verify the competency of our method to extract E_{bw}.

Summary

The blast wave energy conversion efficiency was measured in a quiescent air and in a M = 2 flow. As a result, the efficiency was found to decrease with the decrease in the ambient pressure while it was insensitive to the other parameters: input laser energy, focusing f-number, and the ambient density. Although the competency of the method to extract the efficiency was verified measuring the maximum over-pressure of the blast wave, no explanation has been proposed for these results in this paper.

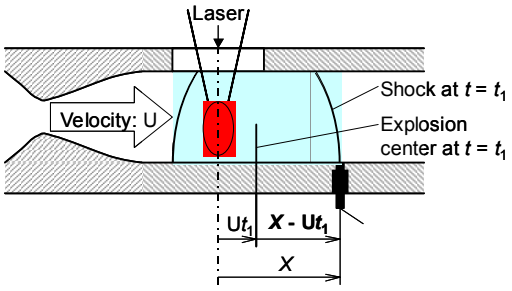

Fig. 11 Convection of the explosion center

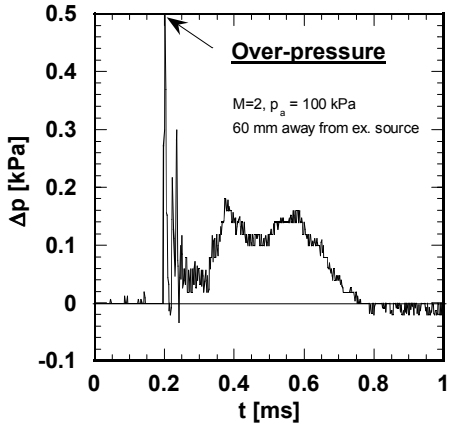

Fig. 12 Temporal history of pressure measured on the bottom surface

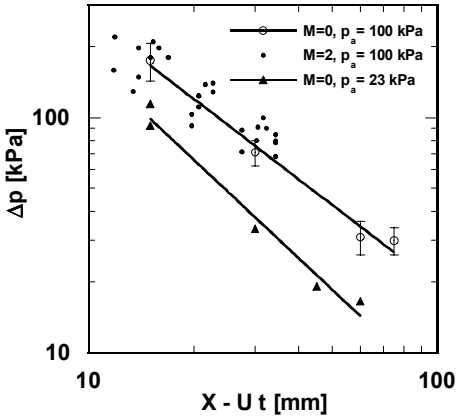

Fig. 13 Relation between the shock radius and the maximum over pressure

References

[1] R. A. Jones, L. N. Myrabo, H. T. Nagamatsu, and M. A. S. Minucci, "Experimental Investigation of an Axisymmetric Hypersonic Scramjet Inlet for Laser Propulsion," Journal of propulsion and power **8**, 1232 (1992).

[2] M. V. Powers, C. L. Zaretzly, and L. N. Myrabo, "Analysis of Beamed-Energy Ramjet/Scramjet Performance," AIAA Paper 86–1761.

[3] H. Katsurayama, K. Komurasaki, and Y. Arakawa, "Computational Performance Estimation of Laser Ramjet Vehicle," AIAA Paper 2002-3778.

[4] Y. P. Raizer, *Laser-Induced Discharge Phenomena, Studies in Soviet Science Consultants Bureau*, New York, 1977, p.199.

[5] P. D. Thomas, "Jet Flowfield behind a Laser-Supported Detonation Wave," AIAA Journal, **15**, 1405 (1977).

[6] V. I. Yakovlev, "Optical Pulsating Discharge Plasma Dynamics in a Supersonic Jet: Experiment and an Analytical Model of the Quasistationary Flow Development," Technical Physics Letters, **27**, 356 (2001).

[7] V. I. Yakovlev, "Supersonic Flow Regimes with a Pulsating Laser Radiation Energy Supply," Technical Physics Letters, **27**, 722 (2001).

[8] J. A. Woodroffe, J.O.A. Stankevics, A. Balantyne, and J. P. Reilly, "Pulsed Laser-Generated Impulse on a Surface in Supersonic Flow," AIAA journal, **18,** 94 (1980)

[9] Sedov, L. I.: Similarity and Dimension Methods in Mechanics (Academic Press, New York, 1959).

[10] A. S. Kompaneets, Soviet Phys. Dokl. **5**, 46 (1960).